Journal of Systemics, Cybernetics and Informatics (2024) 22(2), 48-53
https://doi.org/10.54808/JSCI.22.02.48

Cell Sorting Using Diagonal Bottom Grooves in a Microchannel

Kota YAMAMOTO
Biomedical Engineering, Department of Mechanical Engineering, Kogakuin University
Tokyo, 163-8677, Japan

Shigehiro HASHIMOTO
Biomedical Engineering, Department of Mechanical Engineering, Kogakuin University
at13351@g.kogakuin.jp Tokyo, 163-8677, Japan

ABSTRACT[1]

Cell shape is related to cell function. For the purpose of cell sorting based on shape, a channel with diagonal grooves on the bottom was designed. A cell suspension was poured into a channel created by micromachining, and cell sorting according to shape was confirmed. Experimental results shows that smaller and more elongated cells undergo a larger shift perpendicular to the mainstream direction during passing over the groove. Diagonal bottom grooves in a microchannel are effective for cell sorting.

Keywords: Biomedical Engineering, Cell Sorting, Grooves and Microchannel.

1. INTRODUCTION

Cell sorting is a technology to separate or enrich target cells from a cell population. This technology is widely applied in medical fields such as early cancer diagnosis and regenerative medicine. Flow cytometry [1] is one of cell sorting technologies. In this cell sorting technique, fluorescently labeled antibodies are attached to the cell surface. Cells are identified based on fluorescent signals detected by laser irradiation [2]. This cell sorting technology enables accurate and efficient sorting. However, fluorescent labeling may damage cells [3].

Various label-free (no fluorescent labeling) cell sorting methods have been studied to reduce the risk of cell damage during sorting. Cells were sorted based on differences in various cell characteristics, such as size [4], deformability [5], stiffness [6], and electrical characteristics [7, 8]. Each method has its own merits and demerits, and an appropriate cell sorting method should be selected according to the purpose.

In previous studies, microfluidic channels were fabricated with rectangular microgrooves (inclined at an angle to the flow direction) at the bottom of the channel [9, 10]. It was confirmed that the trajectory of cells changes as they pass over the groove [11, 12]. The possibility of sorting cells using this trajectory change was demonstrated [13, 14].

In this paper, a group of diagonal bottom grooves extending over the full-width in the flow channel has been manufactured. Cells flow movement over the grooves has been tracked to evaluate the capability of grooves for the cell sorting.

2. METHODS

Channel with Bottom Grooves

To change the trajectory of cell motility, microfluidic channels with seven obliquely inclined microgrooves at the bottom (Fig. 1) were fabricated by photolithography technique. The grooves were designed to be 50 μm wide, 60 μm apart, and 5 μm deep. The channel was 2 mm wide, 15 mm long, and 55 μm high (Fig. 2). The grooves are inclined at 45 degrees to the main flow direction.

Photomask

For the base of the photomask of micromachining, a glass plate was used. The glass plate was cleaned by an ultrasonic cleaner. Next, the surface of the glass plate was exposed to oxygen plasma ashing for 5 minutes by RIE-10NR (Samco International, Kyoto, Japan), and chromium was coated on the surface (0.1 μm thick) in an electron beam vapor deposition apparatus (JBS-Z0501EVC, JEOL Ltd., Japan) (Fig. 3).

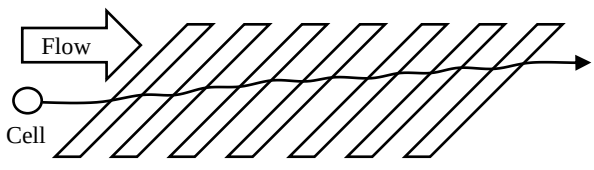

Fig. 1: Grooves at bottom of flow channel for cell sorting.

[1] The authors are grateful to Prof. Richard L. Magin for assistance in the English Editing of this article.

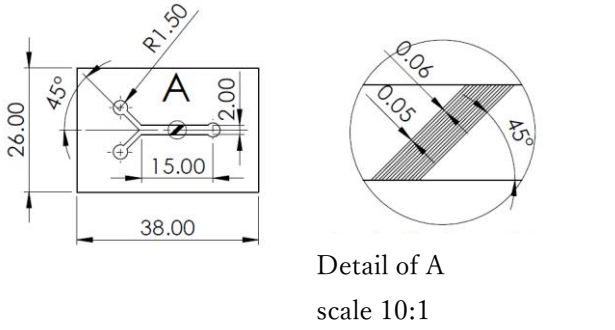

Fig. 2: Dimension (mm) of designed channel with grooves.

To remove dirt such as fingerprints from the surface, the chromium coated surface was cleaned by an ultrasonic cleaner. The photomask was dried by the spin-dryer (with N_2 gas) after cleaning.

To make the surface hydrophilic, the chromium coated surface was exposed to oxygen plasma ashing for 5 minutes by RIE-10NR (Samco International, Kyoto, Japan). In order to improve the adhesion between OFPR-800 (positive resist agent, Tokyo Ohka Kogyo Co., Ltd.) and chromium surface, Hexamethyldisilazane (HMDS, Tokyo Kasei Kogyo Co., Ltd.) was applied using a spin coater (MS-A150, Mikasa Co., Ltd.) at 3000 rpm. The water contained in HMDS was evaporated by heating at 373 K using a hot plate.

The positive photoresist material of OFPR-800LB (Tokyo Ohka Kogyo Co., Ltd, Tokyo, Japan) was coated on the chromium layer with the spin coater (MS-A150, Mikasa Co. Ltd., Tokyo, Japan) at 5000 rpm. The photoresist was baked on the heated plate to evaporate the organic solvent contained in the resist material.

To draw the pattern on the photomask, the laser drawing system (DDB-201K-KH, Neoark Corporation, Hachioji, Japan) was used. In order to improve the performance of the resist material and stabilize the dimensions of the micropattern, the hot plate was used to heat the substrate after exposure.

The photoresist was developed with tetra-methyl-ammonium hydroxide (NMD-3, Tokyo Ohka Kogyo Co., Ltd., Kawasaki, Japan). The OFPR-800 in the exposed area was removed and the micropattern was developed. The photomask was dried by the spin-dryer (with N_2 gas) after the rinse by the ultrapure water.

By immersing the plate in an etching solution (Cr-201, Kanto Kagaku Co., Ltd.) for a specified period of time in a stationary state, only the chromium on the plate on which OFPR-800 is not deposited was etched. To remove OFPR-800 remaining on the substrate, the substrate was ultrasonically cleaned with acetone for 5 minutes and pure water for 5 minutes. The photomask was dried by the spin-dryer (with N_2 gas). The dimension of the stripe patten on the photomask was confirmed by laser microscope (VF-X200, Keyence Corporation).

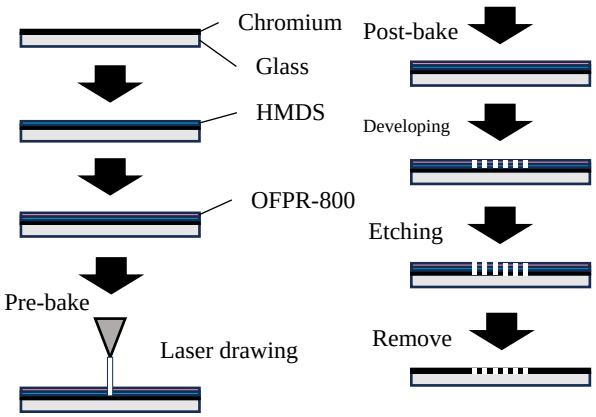

Fig. 3: Photolithography process of photomask.

Lower Plate

The glass plate was used for the base of the mold. To remove dirt such as fingerprints from the surface, the glass surface was cleaned by an ultrasonic cleaner. The plate was dried by the spin-dryer (with N_2 gas) after cleaning. To make the surface hydrophilic, the plate was exposed to oxygen plasma ashing for 5 minutes by RIE-10NR.

The epoxy based negative photo-resist material (SU8-5: Micro Chem Corp., MA, USA) was coated on the glass with the spin coater at a main speed of 2500 rpm (Fig. 4). After the photomask was mounted on the surface of SU8-5, the photoresist was exposed to the ultraviolet (UV) light through the photomask in the mask aligner (M-1S, Mikasa Co. Ltd., Japan). In order to improve the performance of the resist material and stabilize the dimensions of the micropattern, the hot plate was used to heat the substrate after exposure.

The photoresist was developed with SU-8 developer (Nippon Kayaku Co., Ltd, Tokyo, Japan). The micropattern was developed leaving SU8-5 in the exposed area. The glass surface with the micro pattern was rinsed with IPA (2-propanol, Wako Pure Chemical Industries, Ltd.).

In order to improve the adhesion between the substrate and the resist material (SU8-5), the substrate is heated using a hot plate. After the plate was enclosed with a peripheral wall of polyimide tape, PDMS was poured with the curing agent on the plate.

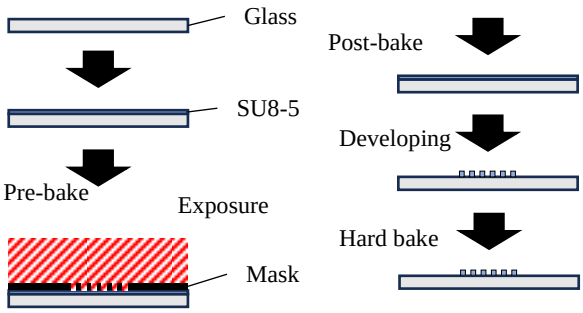

Fig. 4: Photolithography process of mold for lower plate.

Upper Plate

The polyimide tape (0.055 mm thickness) was pasted on the glass plate to make the mold of flow channel pattern for the mold (Fig. 5). After the plate was enclosed with a peripheral wall of polyimide tape, polydimethylsiloxane (PDMS, Sylgard 184 Silicone Elastomer Base, Dow Corning Corporation) was poured with the curing agent on the plate. Holes (diameter of 3 mm) were made for the inlet and the outlet of the channel.

Fig. 5: Mold for upper plate of flow channel.

Both the upper and the lower PDMS plates were exposed to the oxygen gas in the reactive ion etching system (RIE-10NR). Immediately after ashing, the upper disk adheres to the lower disk to make the flow channel (Fig. 2) with 0.055 mm high between them. The inlet and outlet tubes (silicone) were connected to the hole of the upper plate and fixed by additional PDMS (Fig. 6). The flow channel is placed on the stage of an inverted phase-contrast microscope.

Cell Flow Test

The C2C12 cell line (passage < 10, mouse myoblast cells, which originated with cross-striated muscle of C3H mice) was used in the test. Cells were suspended in the D-MEM (Dulbecco's Modified Eagle's Medium). When the cells were aggregated, 0.25% (w/v) Trypsin/0.53 mM (0.2g) EDTA was added little by little to make the cells into a single cell state.

The phosphate buffer solution was prefilled into the channel. Cell suspension (50000 cells/cm^3) was introduced into the flow channel using a syringe pump (0.4 mL/hour) (Fig. 7). The level of inlet chambers were adjusted so that the sheath (medium) flow rate was not slower than the sample flow rate (cell suspension flow). Cells movement was observed by a microscope. The camera (DSC-RX100M4, Sony Corporation) was placed on the eyepiece of the microscope. The behavior of cells passing near the groove was recorded as a video image (frame rate of 30 fps, shutter speed of 1/1250 s).

Fig. 6: Flow channel with tubes.

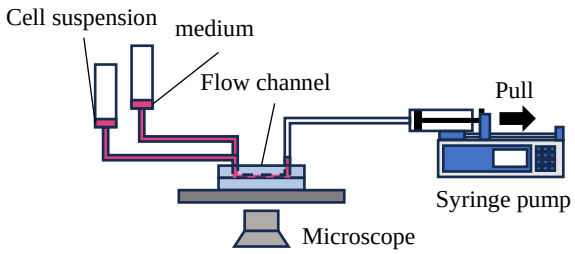

Fig. 7: Experimental system.

Image Analysis

In the two dimensional microscopic image, the coordinates are defined as follows: the direction of main flow is *x*, the direction perpendicular to the main flow is *y* (Fig. 8). "ImageJ" was applied to track each cell. Contour of each cell was traced (Fig. 9). The area surrounded by contour was calculated as *S*. The contour was approximated to ellipse (Fig. 10). The centroid of each cell was tracked to analyze the cell flowing movement over grooves (Fig. 8). While passing over the diagonal grooves, the average diameter *dm* of the cell was calculated from the major axis *a* and the minor axis *b* (Fig. 10).

$$dm = \sqrt{(a \ \ b)} \tag{1}$$

To evaluate the cell shape, the shape index *P* was calculated by Eq (2). For a circle, *P*=0, and as the ellipse gets longer, *P* approaches 1. The mean value of *P* during passing over the groove is calculated as *Pm*.

$$P = 1 - (b / a) \tag{2}$$

Using the coordinates (x, y) of the cell centroid, the cell velocity v of the time (Δt) was calculated by Eq (3).

$$v = (\sqrt{((x_2 - x_1)^2 + (y_2 - y_1)^2)}) / \Delta t \quad (3)$$

where (x_1, y_1) and (x_2, y_2) are the coordinates of the cell centroid at the time of Δt. The mean velocity is defined as vm.

For each cell, the shift movement (perpendicular to the mainstream direction) per groove (Δy) is calculated using Eq (4) from the centroid coordinates y_k after passing through k grooves and the centroid coordinates before the first groove y_0.

$$\Delta y = (y_k - y_0) / k \quad (4)$$

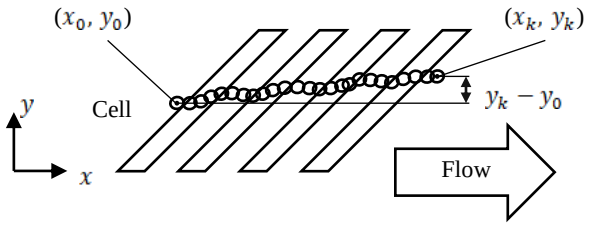

Fig. 8: Coordinates for cell tracking.

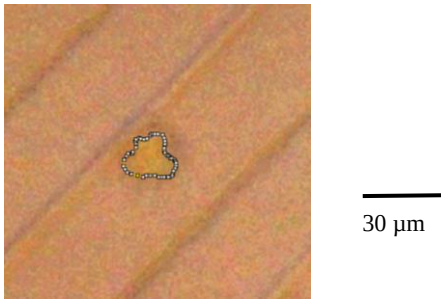

Fig. 9: Traced contour of cell in oblique groove.

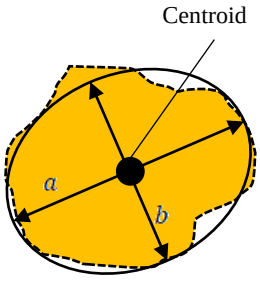

Fig. 10: Contour of cell is approximated to ellipse.

3. RESULTS

Fig. 11 shows the relationship between the shift (Δy) and the mean projected area (Sm) during passing diagonal bottom grooves. A regression line and a correlation coefficient r have been calculated. The vertical displacement (Δy) decreases with the projected area Sm of the cell.

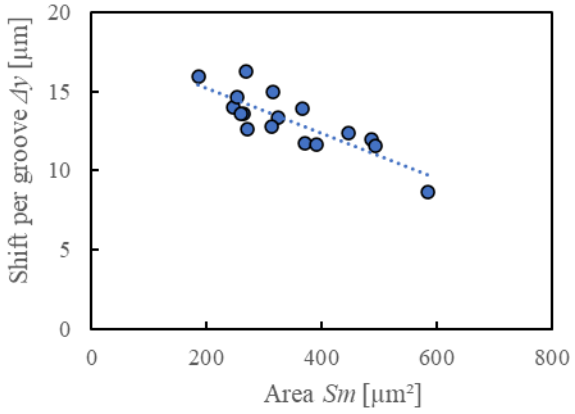

Fig. 11: Relationship between shift per groove Δy and projected area Sm: $\Delta y = -0.014\ Sm + 18$, $r = -0.83$.

Fig. 12 shows the relationship between the shift (Δy) and the cell size (dm) when $k = 4$. Smaller cells have a larger change in direction of movement when passing over the diagonal groove. This tendency can be used to sort cells based on their size.

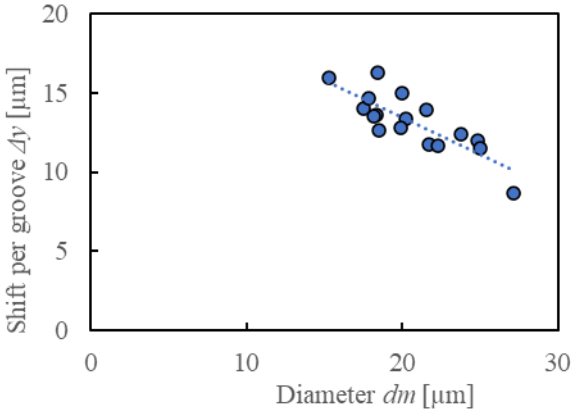

Fig. 12: Relationship between shift per groove Δy and cell diameter dm: $\Delta y = -0.48\ dm + 23$, $r = -0.83$.

Fig. 13 shows the relationship between the shift (Δy) and the shape index (P). It was found that the larger of the shape index, the larger the shift tended to be. The elongated shape has a greater vertical displacement.

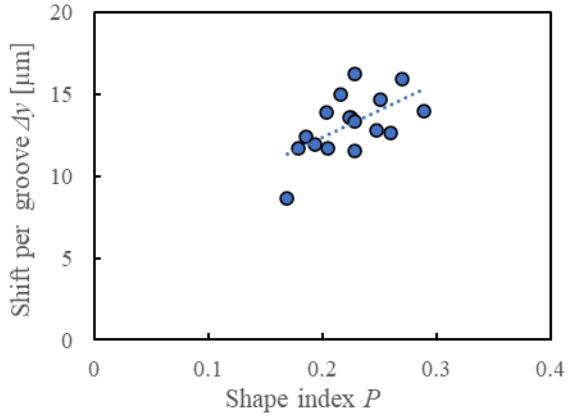

Fig. 13: Relationship between shift Δy per groove and shape index P: $\Delta y = -33\ P + 5.7$, $r = 0.60$.

Fig. 14 shows the relationship between the shift (Δy) and the mean of the cell velocity (v). The higher the cell velocity, the smaller the shift tends to be. A flow rate limitation is necessary for cell sorting.

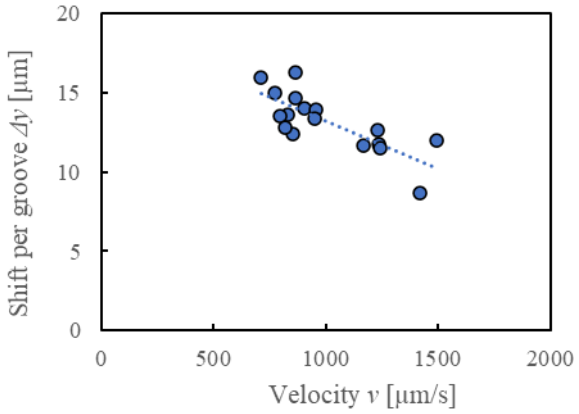

Fig. 14: Relationship between shift per groove and cell velocity: $\Delta y = -0.0060\ v + 19$, $r = -0.78$.

4. DISCUSSION

Shapes that are smaller and farther from the sphere shift more on the groove. Higher speeds result in fewer shifts. A somewhat slower flow is more advantageous for cell separation operations.

In the channel created in this study, cells shift in the positive y direction occurred as they passed over the grooves (Fig. 8). In order to adjust the initial position of the cells, the introduction position of the cell suspension was set to a position with a small y. A sheath flow was introduced in the direction with larger y [15].

The streamlines close to the bottom of the channel bend within the groove in the longitudinal direction of the groove. On the other hand, at the center of the flow path, the influence of bending is smaller and the flow approaches the mainstream direction. When cells are small and flow close to the bottom of the channel, they are guided in the direction of streamlines close to the bottom, and the shift distance in the y direction is larger.

The depth of the bottom groove in our device is less than half the average diameter of floating cells. In this study, cells with reduced adhesion to the bottom of the culture dish were used. It has been reported that the movement during passage over the diagonal groove is related to cell deformation [16]. As a next step, it is expected that this device will be applied to sorting cells based on their activity.

5. CONCLUSIONS

With the aim of designing a microchannel device for cell sorting that causes minimal invasive damage to cells, a microchannel device with seven grooves tilted at 45 degrees to the main channel direction on the bottom surface was fabricated. The experimental results showed that the smaller and more elongated cells had a larger shift perpendicular to the mainstream direction during passage over the groove. To induce a larger shift, the flow velocity should be controlled.

REFERENCES

[1] C. Wang, Y. Ma, Z. Pei, F. Song, J. Zhong, Y. Wang, X. Yan, P. Dai, Y. Jiang, J. Qiu, M. Shi and X. Wu, "Sheathless Acoustic Based Flow Cell Sorter for Enrichment of Rare Cells", **Cytometry A**, Vol. 101, No. 4, 2022, pp. 311-324. https://doi.org/10.1002/cyto.a.24521

[2] M. Brown and C. Wittwer, "Flow Cytometry: Principles and Clinical Applications in Hematology", **Clinical Chemistry**, Vol. 46, No. 8, 2000, pp. 1221-1229.

[3] D. R. Gossett, W. M. Weaver, A. J. Mach, S. C. Hur, H. T. K. Tse, W. Lee, H. Amini and D. D. Carlo, "Label-free Cell Separation and Sorting in Micro-fluidic Systems", **Analytical and Bioanalytical Chemistry**, Vol. 397, No. 8, 2010, pp. 3249-3267. https://doi.org/10.1007/s00216-010-3721-9

[4] K. Matsuura and K. Takata, "Blood Cell Separation Using Polypropylene-Based Microfluidic Devices Based on Deterministic Lateral Displacement", **Micromachines**, Vol. 14, No. 2, 2023, 238. https://doi.org/10.3390/mi14020238

[5] G. Choi, R. Nouri, L. Zarzar and W. Guan, "Micro-fluidic Deformability-activated Sorting of Single Particles", **Microsystems and Nanoengineering**, Vol. 6, No. 11, 2020.

https://doi.org/10.1038/s41378-019-0107-9
[6] G. Wang, W. Mao, R. Byler, K. Patel, C. Henegar, A. Alexeev and T. Sulchek, "Stiffness Dependent Separation of Cells in a Microfluidic Device", **PLOS ONE**, Vol. 8, No. 10, 2013, e75901. https://doi.org/10.1371/journal.pone.0075901
[7] M. Aghaamoo, B. C. Benitez and A. P. Lee, "A High-Throughput Microfluidic Cell Sorter Using a Three-Dimensional Coupled Hydrodynamic-Dielectrophoretic Pre-Focusing Module", **Micromachines**, Vol. 14, No. 10, 2023, 1813. https://doi.org/10.3390/mi14101813
[8] S. Hashimoto and R. Ono, "Dielectrophoretic Movement of Cell Passing Between Surface Electrodes in Flow Channel", **ASME Journal of Engineering and Science in Medical Diagnostics and Therapy**, Vol. 7, No. 2, 2024, pp. 1-7.
[9] S. Hashimoto, "Oblique Micro Grooves on Bottom Wall of Flow Chanel to Sort Cells", **Proc. ASME Fluids Engineering Division Summer Meeting (FEDSM2020)**, 2020, pp. 1-6.
[10] Y. Takahashi, S. Hashimoto, Y. Hori, and T. Tamura, "Sorting of Cells Using Flow Channel with Oblique Micro Grooves", **Proc. 22nd World Multi-Conference on Systemics Cybernetics and Informatics**, Vol. 2, 2018, pp. 138-143.
[11] S. Hashimoto, T. Matsumoto, Y. Endo, S. Kuwabara, H. Yonezawa and K. Yoshinaka, "Velocity of Flowing Myoblast Cell at Oblique Micro Grooves", **Proc. 24th World Multi-Conference on Systemics Cybernetics and Informatics**, Vol. 2, 2020, pp. 31-36.
[12] S. Hashimoto, "Behavior of Cell Flowing Over Oblique Microrectangular Groove", **ASME Journal of Engineering and Science in Medical Diagnostics and Therapy**, Vol. 5, No. 4, 2022, pp. 1-8.
[13] S. Hashimoto, T. Matsumoto and S. Uehara, "How Does a Cell Change Flow Direction Due to A Micro Groove?", **Journal of Systemics, Cybernetics and Informatics**, Vol. 19, No. 8, 2021, pp. 164-181.
[14] S. Hashimoto and H. Yonezawa, "Movement of Cell Flowing Over Oblique Micro Grooves in Flow Channel", **Proc. ASME Fluids Engineering Division Summer Meeting (FEDSM2021)**, 2021, pp. 1-7.
[15] K. Yamamoto and S. Hashimoto, "Design of Flow Channel for Cell Sorting by Size and Deformability", **Proc. 27th World Multi-Conference on Systemics Cybernetics and Informatics**, Vol. 1, 2023, pp. 57-60.
[16] S. Hashimoto, S. Uehara and N. Moriizumi, "Movement of Cell Flowing over Oblique Microgroove", **Journal of Systemics, Cybernetics and Informatics**, Vol. 21, No. 1, 2023, pp. 73-79.